110th Anniversary: Near-Total Epoxidation Selectivity and Hydrogen Peroxide Utilization with Nb-EISA Catalysts for Propylene Epoxidation

Swarup K. Maiti,[†] Anand Ramanathan,[†] and Bala Subramaniam*,[†,‡]

[†]Center for Environmentally Beneficial Catalysis, University of Kansas, Lawrence, Kansas 66047, United States
[‡]Department of Chemical and Petroleum Engineering, University of Kansas, Lawrence, Kansas 66045, United States

S *Supporting Information*
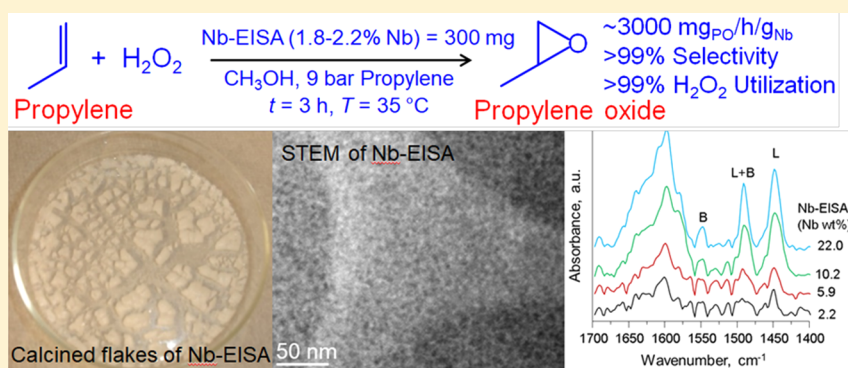
ABSTRACT: The Nb-EISA catalyst with relatively low Nb loadings (~2 wt %) shows exceptional propylene epoxidation performance with H_2O_2 as oxidant at 30−40 °C, 5−9 bar propylene pressure with nearly total propylene oxide (PO) selectivity (>99%), H_2O_2 utilization (>99%) toward PO formation, high productivity (~3200 mg/h/g), and mild Nb leaching (3−6%). The predominantly Lewis acidic nature of the Nb-EISA catalysts favors epoxidation while their relatively low Brønsted acidity inhibits H_2O_2 decomposition and Nb leaching. At higher Nb loadings (8−17 wt %), the catalytic performance deteriorates. However, significant performance improvements were achieved when the Nb-EISA materials are calcined in N_2 (instead of air) during synthesis, depositing a carbon layer in the pores. The resulting pore hydrophobicity not only inhibits epoxide ring opening but also increases propylene concentration inside the pores resulting in higher EO productivity and lower H_2O_2 decomposition. The carbonized Nb-EISA materials also show improved stability to leaching.

1. INTRODUCTION

Propylene oxide (PO) is one of the most important chemical intermediates for producing many essential fine chemicals, such as polyurethane plastics, polyglycol esters, unsaturated resins, and surfactants.[1−3] The global demand for PO is high, being >10 million metric tons/year in 2012 and growing at an annual rate of 5%.[4,5] In general, PO is produced via epoxidation of propylene, an industrially significant substrate. Current commercial routes to PO production are mainly the chlorohydrin process, different hydroperoxide based processes, and the hydrogen peroxide propene oxide (HPPO) process. While the chlorohydrin process suffers from high environmental impact due to much waste generation, the hydroperoxide-based processes depend on stable byproduct (*tert*-butyl alcohol) value for economic viability. Among these processes, the HPPO process has less environmental impact as it produces only H_2O as byproduct and uses mild operating conditions (40−50 °C and 20−30 bar). The HPPO process provides a maximum PO selectivity of 95% using the titanium silicate (TS-1) catalyst[6−8] in methanol solvent. While the TS-1

catalyst is active, it is expensive and undergoes deactivation.[9] Further, the extent to which H_2O_2 decomposes on the acidic TS-1 catalyst is unknown. Stoichiometric utilization of H_2O_2 toward PO formation with near-complete PO selectivity is vital to making the process economically viable. Hence, there continues to be interest in alternative PO processes using inexpensive and robust catalysts that maximize PO selectivity and H_2O_2 utilization.

Various catalysts have been investigated for propylene epoxidation with hydrogen peroxide, including heteropolya-cids,[10,11] methyltrioxorhenium (MTO),[9] tungsten based homogeneous catalysts,[12] and various titanium containing zeolites, viz., Ti-MWW[13] and $TiCl_4$-modified HZSM-5,[14] in addition to TS-1.[6−8] For example, Xi et al. performed propylene epoxidation[10] at 65 °C using *in situ* formed H_2O_2

with 85% PO yield in a 6 h batch run. The catalyst, $[\pi\text{-}C_5H_5NC_{16}H_{33}]_3[PO_4(WO_3)_4]$, used in this system is insoluble but can form a soluble active species in the presence of H_2O_2. When the H_2O_2 is consumed, the catalyst precipitates enabling easy recycling. Lee et al. developed a liquid phase propylene epoxidation process[9] using the MTO catalyst under mild operating conditions similar to those of the HPPO process producing PO with 98% yield and complete H_2O_2 utilization for PO formation. In contrast, most of the Ti-based heterogeneous catalysts show lower H_2O_2 utilization toward PO formation compared to MTO. For example, the H_2O_2 utilization toward PO formation is reported to be 94% and 96% respectively over Ti-MCM-42 and Ti-MWW catalysts. These Ti-based catalysts are often tedious and expensive to synthesize. Similar to Ti, Nb-[15−30] and W-based catalysts[21,29] are also active for olefin epoxidation using H_2O_2 as oxidant. However, in studies of liquid-phase ethylene epoxidation with H_2O_2, we found that metal leaching is a major problem being more severe for W[29] in general compared to Nb-based silicates.[21]

The epoxidation activity of Nb-silicates is in general attributed to the presence of well dispersed Nb(V) sites in tetrahedral coordination. We demonstrated recently that improved Nb dispersion can be achieved using the Evaporation Induced Self-Assembly (EISA) synthesis method with relatively low Brønsted acidity. The Nb-EISA catalysts show remarkable activity for cyclohexene epoxidation with high epoxidation selectivity compared to Nb-catalysts prepared by either one-pot or impregnation methods.[31] Further, carbonization of the Nb-EISA catalyst[31] via calcination in the presence of N_2 remarkably stabilizes the epoxide from ring opening reactions while also improving H_2O_2 utilization toward epoxide formation.

Invariably almost all reported epoxidation studies with Nb-based catalysts involve substrates such as cyclohexene, cyclooctene, limonene, and vegetable oil that are liquids at ambient conditions. Our work addresses the important question of how these epoxidation catalysts fare in the case of a lower olefin such as propylene that requires higher pressures to ensure adequate solubility in the liquid phase. As propylene (P_c = 46 bar, T_c = 92.2 ± 0.8 °C) is close to its critical temperature at ambient conditions, it dissolves significantly in the liquid phase containing methanol (as in the HPPO process and our experiments) depending on the pressure. This causes the volume of the liquid phase to change with pressure, which must be experimentally quantified to reliably design experiments and to interpret the results. In the only reported study of Nb-based heterogeneous catalyst for liquid phase epoxidation of propylene, such important details are not addressed.[32]

Motivated by the foregoing considerations, we report here systematic investigations of Nb-EISA catalysts and their carbonized versions, C−Nb-EISA, for propylene epoxidation under similar operating conditions as those employed in the HPPO process. Remarkably, the Nb-EISA catalysts show exceptional propylene epoxidation activity, stability, and H_2O_2 utilization compared to Nb-silicates prepared by other one-pot and impregnation methods. Optimized Nb-EISA catalysts perform significantly better for propylene epoxidation than Ti-based catalysts providing >99% epoxide selectivity and H_2O_2 utilization.

2. EXPERIMENTAL SECTION

2.1. Materials. Triblock copolymer (Pluronic P123, EO_{20}−PO_{70}−EO_{20}, with an average molecular weight ∼5,800, Aldrich), ethanol (Absolute, 200 Proof, Acros organics), methanol (Sigma-Aldrich), tetraethyl orthosilicate (TEOS) (98% Acros organics), conc. hydrochloric acid (37%, Fisher), and niobium(V) chloride (Alfa Aesar) were used as received. Acetonitrile (HPLC grade, 99.9%, Fisher) and H_2O_2 (50 wt % in water, Fisher) were used as received for catalytic propylene epoxidation with H_2O_2. Ferroin indicator solution, ceric sulfate (0.1 N), and trace metal grade sulfuric acid (99.9 wt %) were purchased from Fischer Scientific and used as received. The PO standard, 1-methoxy-2-propanol, and propylene glycol were purchased from Sigma-Aldrich, whereas 2-methoxy-1-propanol was purchased from Chem-Bridge Chemical. Propylene was purchased from Matheson Tri-Gas Co (polymer grade).

2.2. Synthesis of Nb-EISA and Catalyst Characterization. The Nb-EISA catalysts were prepared as described previously.[31] Briefly, TEOS was added to the acidified ethanolic solution containing P123, followed by the required amounts of niobium(V) chloride predissolved in ethanol. After stirring the mixture for a couple of hours, it is transferred to a Pyrex Petri dish, and the solvent is allowed to evaporate for 2−4 days. The resulting rigid flakes were then calcined in either flowing air or nitrogen at 550 °C for 5 h at a heating rate of 1.5 °C/min to obtain either Nb-EISA or Nb-EISA, respectively. The calcined samples were characterized with a comprehensive suite of complementary analytical techniques including SAXS, XRD, XRF, N_2 physisorption, diffuse reflectance UV−vis spectroscopy, transmission electron microscopy (TEM, SEM), NH_3-TPD, and FTIR of adsorbed pyridine.[31]

The metal contents in the fresh and spent solid catalysts were determined by inductively coupled plasma optical emission spectrometry (ICP-OES). Prior to analysis, the catalyst (60 mg) was digested in the presence of HF (2 g), H_2SO_4 (3 g), and deionized water (5 g) in an autoclave at 100 °C for 3 h. The resulting solutions were analyzed by the ICP-OES technique using appropriate calibration standards. The ICP-OES analysis offers high sensitivity in calculating metal concentrations in the catalysts (±1.6 ppm for Nb and ±0.78 ppm for Si).

2.3. Volumetric Expansion Studies. When pressurized propylene is dissolved in methanol, it shows enhanced solubility resulting in propylene-expanded liquids. A 50 mL high-pressure Jerguson cell rated to ∼400 bar at 100 °C[33] was used for volumetric expansion studies. Either pure methanol or a methanol + 50% H_2O_2/H_2O mixture is placed in the view cell which is then submerged in a constant temperature bath. To facilitate the mixing of cell contents, the loaded liquid is agitated by a piston. Once the desired temperature is attained, propylene is pumped as a liquid from an ISCO pump into the cell to the desired pressure. Mixing of the gas and liquid phases by a piston expedites the attainment of equilibrium (as inferred from constant P and T). At equilibrium, the volume of a propylene expanded liquid phase is measured visually on a calibrated external linear scale.

2.4. Catalytic Epoxidation Studies. The catalysts were tested for propylene epoxidation in a semibatch mode in a 50 mL Parr reactor equipped with a magnetically driven stirrer, pressure transducer, and thermocouple. Reactor details and the operating procedure are described elsewhere,[21] and a

schematic of the reactor unit is given in the Supporting Information (Figure S1). In a typical reaction, a mixture containing a 50% aqueous H_2O_2 (10 mmol) solution, MeOH (625 mmol), acetonitrile (3 mmol) as internal standard, and a solid catalyst (fresh or spent) was loaded into the Parr reactor. A blank experiment using 1,2-dimethoxyethane (DME) as internal standard confirmed the inertness of acetonitrile. The solution was heated with mild stirring to attain the desired temperature (35 °C). Thereafter, propylene was charged from an external reservoir pressurizing the reactor up to 0.9 MPa. The impeller speed was kept at 1400 rpm to eliminate gas–liquid mass transfer limitations. Isothermal semibatch reactions lasting up to 3 h were performed at constant pressure. The liquid-phase reaction mixture was analyzed by online GC to determine the concentrations of the desired product (PO) and the byproducts [1-methoxy-2-propanol (1M2P), 2-methoxy-1-propanol (2M1P), and propylene glycol (PG)]. The following definitions are used in evaluating the performance of the tested catalysts

$$P_{PO} = \frac{m_{PO}}{(\text{batchtime})(m_{metal})}$$

$$S_{PO} = \left(\frac{n_{PO}}{n_{PO} + n_{1M2P} + n_{2M1P} + n_{PG}} \right) \times 100\%$$

$$U_{H_2O_2} = \frac{n_{PO} + n_{1M2P} + n_{2M1P} + n_{PG}}{n_{H_2O_2}^0 - n_{H_2O_2}} \times 100\%$$

$$X_{H_2O_2} = \frac{n_{H_2O_2}^0 - n_{H_2O_2}}{n_{H_2O_2}^0} \times 100\%$$

where P_{PO}, S_{PO}, $U_{H_2O_2}$, and $X_{H_2O_2}$ denote PO productivity (mg PO h^{-1} g^{-1} metal), PO selectivity, H_2O_2 utilization toward PO formation, and H_2O_2 conversion, respectively; m_{PO} and m_{metal} represent the mass of PO formed and the mass of metal in the catalyst, respectively; n_{PO}, n_{1M2P}, n_{2M1P}, and n_{PG} denote the molar amounts of PO, 1M2P, 2M1P, and PG formed, respectively; and $n_{H_2O_2}^0$ and $n_{H_2O_2}$ denote the initial and the final molar amounts of H_2O_2, respectively.

3. RESULTS AND DISCUSSION

3.1. Catalyst Characterization. Detailed physicochemical characterization of Nb-EISA samples and their carbonized versions (C−Nb-EISA) may be found in the Supporting Information (Figures S2−S9) and elsewhere.[31] Only the salient features are summarized here. The mesoporous nature of Nb-EISA and C−Nb-EISA samples was confirmed by N_2 sorption revealing typical type IV isotherm and H_2 hysteresis. The physicochemical characteristics are summarized in Table 1. For Nb-EISA and C−Nb-EISA samples, the surface area ranges from 615 to 680 m^2/g and from 418 to 571 m^2/g, respectively, decreasing with increased Nb content (1.6−22.0 wt %). These materials possess an average pore diameter of about 2.7−3.4 nm. Further, the total acidity (0.10−0.31 mmol NH$_3$/g) was found to be lower compared to other Nb containing mesoporous silicates. Although an increase in the relative amounts of Lewis acid sites was inferred from the FTIR spectra of adsorbed pyridine, relatively low amounts of Brønsted acid sites were observed (Table 1). Further, the weak Brønsted acidity is confirmed by complete desorption of pyridine at mild temperature (250 °C). Diffuse reflectance

Table 1. Physical Properties of Nb-EISA and C−Nb-EISA Catalysts

no.	catalyst	Nb wt %[a]	C wt %[b]	S_{BET}[c] (m^2/g)	V_{tp}[d] (cm^3/g)	$d_{P, BJH}$[e] (nm)	acidity NH$_3$ (mmol/g)
1	Nb-EISA	1.8		680	0.45	3.0	0.10
2		3.7		618	0.46	3.4	0.18
3		6.0		962	1.11	4.6	0.18
4		10.2		681	0.54	3.4	0.24
5		22.0		615	0.47	3.4	0.31
6	C−Nb-EISA	1.6	16.5	571	0.40	2.9	0.06
7		3.3	21.5	473	0.36	2.9	0.12
8		7.8	23.4	426	0.41	3.2	0.18
9		16.6	24.7	418	0.37	3.2	0.22
10	Nb-EISA[f]	1.9		557	0.36	2.7	ND[j]
11	Nb-EISA[g]	1.8		549	0.35	2.7	ND[j]
12	Nb-EISA[h]	1.4		512	0.32	2.7	ND[j]
13	C−Nb-EISA[i]	1.4	NM[i]	555	0.41	2.9	ND[j]

[a]wt % in sample determined by XRF. [b]wt % in sample determined by TG/DTA. [c]S_{BET} = BET specific surface area from adsorption isotherm at P/P_0 between 0.05 and 0.30. [d]V_{tp} = total pore volume at 0.99 P/P_0. [e]$d_{P,BJH}$ = average pore diameter calculated from adsorption branch of N_2 isotherms using the BJH model. [f]Another batch of Nb-EISA (1.9%). [g]After 10 h reaction. [h]After 4 recycle runs. [i]NM = not measured. [j]ND = not determined.

UV−vis characterization reveals the presence of bands at 200−204 nm attributed to ligand-to-metal charge transfer in isolated NbO$_4$ tetrahedra and another band at 242−267 nm due to oligomeric NbO$_x$ tetrahedral.[31] The lack of a band at 290−320 nm implies the absence of bulk Nb$_2$O$_5$ species which is also evidenced from powder XRD patterns.[31]

3.2. Volumetric Expansion Studies. While conventional liquid phases are noncompressible, gas-expanded liquid phases are compressible. The compressibility depends on the extent of gas dissolution in the liquid phase. Hence, volumetric expansion data are important to calculate the propylene concentration in the liquid phase precisely. Such data also facilitate reliable interpretation of the effects of various parameters such as temperature, propylene pressure, and aqueous H_2O_2 concentration on the extent of dissolution of propylene in the liquid phase. As shown in Figure 1, the volume of initial liquid phase containing either pure methanol or a representative reaction mixture (containing methanol and
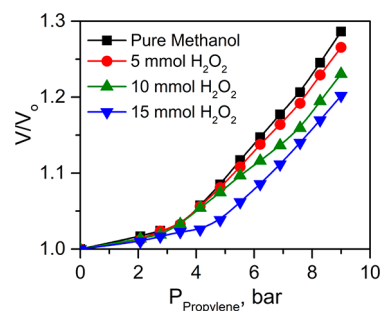
Figure 1. Volumetric expansion plot with propylene pressure at 35 °C.

Table 2. Performances of Nb-EISA with Different Nb Loadings and Reaction Times for Propylene Epoxidation[b]

no.	Nb-EISA, Nb wt %	time (h)	Y_{PO} (mmol) (±3%)	P_{PO} (±3%)	S_{EO} % (±3%)	$X_{H_2O_2}$ % (±3%)	$U_{H_2O_2}$ % (±3%)	leaching % (±5%)
1	1.8[a]	3	0.63	2340	>99	5.3	>99	3.5
2	3.7	3	1.20	2071	>99	12.7	94.5	5.4
3	6.0	3	2.84	3050	>99	28.7	96.3	9.3
4	10.2	3	1.23	777	91.8	22.7	59.0	13.7
5	22.0	3	0.84	247	86.6	31.5	31.1	4.5
6	2.0[a]	3	0.94	3171	>99	9.1	>99	3.5
7	2.0[a]	10	2.85	2900	>99	27.9	>99	5.7
8	1.9[a]	3	0.93	3174	>99	9.3	>99	3.3

[a]Different batches with similar Nb loadings. [b]Reaction conditions: MeOH = 624 mmol, H_2O_2 = 10 mmol, AN = 3 mmol, catalyst loading = 300 mg, T = 35 °C, propylene P = 9 bar (maintained constant), 1400 rpm.

50% aqueous H_2O_2) increases with increasing propylene pressure, implying increased propylene dissolution in the liquid phase. At a fixed temperature, the extent of volumetric expansion decreases with increasing H_2O_2 concentration in the methanol + H_2O_2 (50% aqueous) mixture. At 35 °C and 9 bar propylene pressure, the volumetric expansion in the case of pure methanol is 29%. In the case of methanol + H_2O_2 (aqueous) mixtures, the volumetric expansion caused by propylene dissolution at 9 bar and 35 °C is 27%, 23%, and 20% when the H_2O_2 contents in the mixture are 5, 10, and 15 mmol, respectively. As expected, increased concentrations of polar H_2O_2 in the liquid phase decrease the solubility of nonpolar propylene. Even though the main product, PO, was not included in the volumetric expansion studies, PO formation during reaction (3 h) constitutes only ~0.8 wt % of the reaction mixture and, hence, is not expected to alter the propylene dissolution significantly.

3.3. Epoxidation of Propylene. *3.3.1. Epoxidation of Propylene by Nb-EISA Catalysts.* Nb-EISA catalysts with different Nb loadings were screened for propylene epoxidation, and the results are summarized in Table 2 (entries 1−5). The Nb-EISA catalyst with 1.8 wt % Nb loading displayed nearly total S_{PO} (>99%) and $U_{H_2O_2}$ (>99%) with relatively low Nb leaching (3.5%) during a 3 h run. With an increase in Nb loading up to 10.2 wt %, the yield of PO increased and then decreased at the high Nb loading of 22 wt %. $U_{H_2O_2}$ values also decreased with increased Nb loading. The decreases in P_{PO} and $U_{H_2O_2}$ values at the higher Nb loadings are attributed to the formation of oligomeric NbOx species that are not as active as the isolated NbOx species for epoxidation. Further, the Brønsted acidic nature of the oligomeric NbOx species also decomposes H_2O_2, adversely affecting its utilization for PO formation.

We prepared different batches of Nb-EISA materials with similar Nb loadings (1.9−2.0 wt %) and tested for catalyst stability during extended runs (Table 2, entries 6−8). Similar P_{PO} was observed for the extended run (10 h) suggesting that the catalyst is stable under the reaction conditions. Further, the decreased Nb leaching (5.7% at 10 h vs 3.5% at 3 h) does not scale with reaction time suggesting that the leaching decreases with time. Additionally, Nb-EISA catalysts prepared in two different batches with almost identical Nb loadings show similar catalytic activities (Table 2, entries 6 and 8) under similar reaction conditions. This indicates that the catalyst synthesis technique is reproducible for similar Nb loadings.

We also tested various mesoporous Nb-silicate catalysts (viz., Nb-KIT-5, Nb-KIT-6, and Nb-TUD-1) that were active for ethylene epoxidation.[21,29] As shown in Table 3 (entry 1),

Table 3. Performances of Different Nb-Silicates for Propylene Epoxidation[b]

no.	catalyst	Nb wt %	P_{PO} (±3%)	S_{EO} % (±3%)	$X_{H_2O_2}$ % (±3%)	$U_{H_2O_2}$ % (±3%)	leaching % (±5%)
1	Nb-KIT-5	2.2	2500	88	15.6	70	10.3
2	Nb-TUD-1	3.8	4075	>99	27.1	89.4	20.9
3	Nb-TUD-1[a]	3.8	3329	>99	26.3	74.6	22.2
4	Nb-TUD-1	0.8	11680	>99	17.0	80.1	24.8
5	Bn-Nb-TUD-1	2.7	907	>99	4.1	93.6	3.6

[a]Reaction temperature is 40 °C. [b]Reaction conditions: MeOH = 624 mmol, H_2O_2 = 10 mmol, AN = 3 mmol, catalyst loading = 300 mg, T = 35 °C, propylene P = 9 bar (maintained constant), t = 3 h, 1400 rpm.

Nb-KIT-5 (2.2 wt % Nb) exhibits moderate PO productivity (P_{PO}) (2500 mg/h/g) and PO selectivity (S_{PO}) (88%). The H_2O_2 utilization efficiency ($U_{H_2O_2}$) is 70%, and the Nb leaching during the 3 h run was 10.3%. In contrast, Nb-TUD-1 (0.8−3.8 wt %) displayed higher P_{PO} (4,075−11,680 mg/h/g) and PO selectivity (S_{PO} > 99%) with moderate to high $U_{H_2O_2}$ (75−90%) values. However, the leaching of Nb-TUD-1 catalysts (20−24%) was more severe compared to Nb-KIT-5 (10%). In the case of Nb-TUD-1 with 3.8 wt % Nb loading, an increase in temperature (from 308 to 313 K) decreases P_{PO} from 4,075 to 3,329 mg/h/g and $U_{H_2O_2}$ from 89.4% to 74.6%, probably due to the decrease of propylene concentration in the liquid phase and/or H_2O_2 decomposition (Table 3, entries 2 and 3). At even lower Nb loadings (0.8 wt %), P_{PO} was significantly enhanced to 11,680 mg/h/g. This is attributed to the dominant presence of Lewis acid sites compared to Brønsted acid sites at low Nb loadings.[21] However, the Nb leaching (~25%) was still significant. Bn-Nb-TUD-1,[30] prepared by covalent capping of benzyl groups on Nb-TUD-1 (3.8 wt % Nb), displayed a better performance than that of the uncapped catalyst with dramatically reduced metal leaching from 21% to 3.6%. However, this capped catalyst showed almost 4-fold less PO productivity (907 vs 4075 mg/h/g) attributed to the reduction of Lewis acid sites during the passivation step.[21] In contrast, the Nb-EISA catalysts show nearly total epoxide selectivity and H_2O_2 utilization with significantly lower Nb leaching (Table 2). This enhanced performance is attributed to the predominance of Lewis acid sites with relatively low Brønsted acidity in the Nb-EISA catalysts.

Table 4. Effect of Temperature, Pressure, H_2O_2 Concentration, and Catalyst Loading for Propylene Epoxidation over Nb-EISA (2.0 wt % Nb)^c

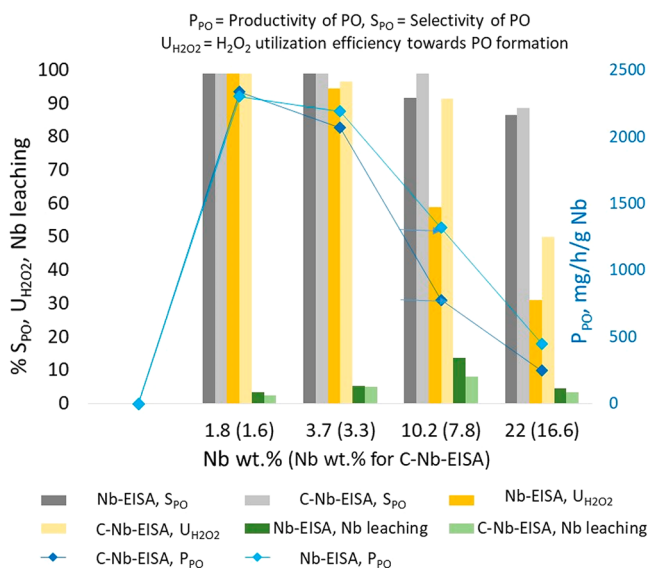| no.	T (°C)	P (bar)	H_2O_2 (mmol)	catalyst amt (mg)	Y_{PO} mmol (±3%)	P_{PO} (±3%)	S_{EO} % (±3%)	$X_{H_2O_2}$ % (±3%)	$U_{H_2O_2}$% (±3%)	leaching % (±5%)
1	30	9	10	300	0.48	1618	>99	4.67	>99	5.2
2	35	9	10	300	0.94	3171	>99	9.08	>99	3.1
3	40	9	10	300	0.83	2809	>99	8.28	97.1	4.9
4	45	9	10	300	0.58	1964	>99	9.04	65.2	4.0
5	35	7	10	300	0.48	1618	>99	4.67	>99	5.2
6	35	5	10	300	0.30	1032	>99	3.0	>99	4.0
7	35	20^a	10	300	0.97	3232	>98	11.4	86	NM^b
8	35	9	5	300	0.22	733	>99	2.2	>99	1.5
9	35	9	15	300	1.41	4776	>99	11.7	80.1	4.0
10	35	9	10	150	0.47	3188	>99	4.5	>99	5.2
11	35	9	10	600	1.21	2052	>99	11.4	>99	3.6
12	35	9	10	900	1.54	1760	>99	14.7	>99	3.8

^{a}9 bar propylene and 11 bar N_2. ^{b}NM = not measured. ^{c}Reaction conditions: MeOH = 624 mmol, AN = 3 mmol, propylene P = maintained constant, t = 3 h, 1400 rpm.

Parametric studies including temperature, propylene pressure, H_2O_2 concentration, and catalyst loading were performed with the Nb-EISA catalyst with 2 wt % Nb, the best-performing catalyst (Table 2). Table 4 summarizes temperature effects. When the reaction temperature is increased from 30 to 35 °C, the PO yield increased approximately 2-fold. Notably, both PO selectivity and H_2O_2 utilization remained high (>99%) at 35 °C. However, at higher temperatures (40 and 45 °C), both PO productivity and H_2O_2 utilization efficiency decreased. The lower activity at higher temperatures (40 and 45 °C) is attributed to the lower propylene dissolution in the gas-expanded liquid phase as well as increased H_2O_2 decomposition, resulting in decreased availability of the two key reactants.

At 35 °C, PO yield increases with propylene pressure. At 35 °C, the PO yields are 0.30, 0.48, and 0.94 mmol at propylene pressures of 5, 7, and 9 bar, respectively (Table 4, entries 2, 5, and 6). Notably, nearly total (>99%) S_{PO} and $U_{H_2O_2}$ were achieved in this pressure range, and Nb leaching remained low (within 3–4%). The increased PO yield at higher propylene pressures is attributed to enhanced propylene solubility in the methanolic liquid phase (Figure 2). Given that propylene at 35 °C is below its critical temperature (92.2 ± 0.8 °C), pressurization with N_2 beyond the saturation vapor pressure would cause propylene condensation and dissolution in the liquid phase. For example, when propylene at 9 bar was pressurized with 11 bar of N_2 at 35 °C, the PO yield increased approximately 10% more (Table 4, entries 2 and 7).

The effect of H_2O_2 concentration was also studied. As inferred in Table 4 (entries 2, 8, and 9), PO productivity increased significantly with an increase in H_2O_2 concentration. However, Nb leaching also increased. While negligible H_2O_2 decomposition was observed when 5 or 10 mmol of H_2O_2 was used, significant H_2O_2 decomposition occurred when 15 mmol of H_2O_2 was used.

When the catalyst loading is increased by 2-fold (from 150 to 300 mg, entries 10 and 2 in Table 4), the PO yield doubled, resulting in similar PO productivity. However, when the catalyst loading was further increased by 4- and 6-fold (from 150 mg to 600 and 900 mg, entries 10–12), the corresponding increases in PO yield were 2.6× and 3.2×, respectively. These are also reflected in the lower PO productivity at higher catalyst loadings (beyond 300 mg). Thus, lower temperature

P$_{PO}$ = Productivity of PO, S$_{PO}$ = Selectivity of PO
U$_{H2O2}$ = H_2O_2 utilization efficiency towards PO formation

Figure 2. Comparative epoxidation performances of Nb-EISA catalysts and its carbonized versions (C−Nb-EISA) at different Nb loadings.

(~35 °C), lower Nb loadings (~2 wt %), and moderate propylene pressure (~9 bar) are preferred to maximize PO productivity and H_2O_2 utilization while minimizing Nb leaching. Figure 2 compares key performance measures of the Nb-EISA catalyst and its carbonized version at different Nb loadings. The figure more clearly displays how carbonized Nb-EISA (C−Nb-EISA) catalysts show better catalytic performance than neat Nb-EISA, becoming more prominent at higher Nb loadings.

3.3.2. Epoxidation of Propylene by Carbonized Nb-EISA Catalysts (C−Nb-EISA). In order to improve H_2O_2 utilization and epoxide selectivity at higher Nb loadings, the as-synthesized Nb-EISA materials were carbonized by calcination in the presence of N_2 (rather than air) at 550 °C. As expected, the C−Nb-EISA (carbonized version of Nb-EISA) catalysts showed better P_{PO}, S_{PO}, $U_{H_2O_2}$, and resistance to metal leaching compared to Nb-EISA with similar Nb loadings (Table 5). For the Nb-EISA catalyst with 10.2 wt % Nb, the values of P_{PO}, S_{PO}, $U_{H_2O_2}$, and Nb leaching were 777 mg/h/g, 92%, 59%, and

Table 5. Performances of C−Nb-EISA with Different Nb Loadings and Reaction Times for Propylene Epoxidation[a]

no.	C−Nb-EISA, Nb wt %	Y_{PO} mmol (±3%)	P_{PO} (±3%)	S_{EO} % (±3%)	$X_{H_2O_2}$ % (±3%)	$U_{H_2O_2}$% (±3%)	leaching % (±5%)
1	1.6	0.55	2305	>99	5.3	>99	2.4
2	3.3	1.12	2193	>99	11.2	96.7	5.0
3	7.8	1.60	1320	>99	16.7	91.4	8.0
4	16.6	1.16	450	88.7	26.7	50.0	3.5

[a]Reaction conditions: MeOH = 624 mmol, H_2O_2 = 10 mmol, AN = 3 mmol, catalyst loading = 300 mg, T = 35 °C, propylene P = 9 bar (maintained constant), 1400 rpm.

13.7%, respectively (Table 2, entry 3), compared to 1320 mg/h/g, >99%, 91%, and 8% observed with C−Nb-EISA catalysts with 7.8 wt % Nb (Table 5, entry 3). We hypothesize that carbonization of the silica matrix induces pore hydrophobicity[34] which in turn enhances the propylene concentration in the pores,[35] resulting in higher propylene epoxidation rates. Further, pore hydrophobicity reduces the concentration of polar molecules such as water inside the pores and therefore mitigates the formation of Brønsted acid sites, a causative factor for H_2O_2 decomposition over Nb silicates.[21] Although the percentage of leached species decreases at the highest Nb loading (16.6 wt %), the absolute amount of Nb leached from this catalyst is more or less the same as the catalyst with 7.8 wt % Nb loading. The population of oligomeric NbOx species (inactive for epoxidation) is progressively greater in catalysts with higher Nb loadings. The oligomeric species are more susceptible to leaching compared to the isolated NbOx species although the rate of leaching appears to taper off at higher loadings.

3.3.3. Catalyst Stability. Recycle tests with the Nb-EISA catalyst with 1.9 wt % Nb loading were carried out up to four cycles (Table 6, entries 1−5). Notably, a slightly improved PO productivity (P_{PO}) was achieved in the first recycle run compared to the first run with a fresh catalyst. Interestingly, after the first recycle run, P_{PO} remained almost unchanged during the subsequent recycle runs. Nearly total PO selectivity and H_2O_2 utilization were observed with steady but low Nb leaching (∼6 wt %) during the recycle runs. The increased PO productivity during the first recycle run may be attributed to the leaching of extra framework NbOx species that are not as active as the framework Nb species. The carbonized version, C−Nb-EISA with 1.55 wt % Nb loading, showed similar trends

during four recycle runs (Table 6 entries 6−10), confirming that both Nb-EISA and its carbonized version are recyclable catalysts.

During allyl alcohol epoxidation with hydrogen peroxide, both Ti-MCM-41 and Ti-SBA-15 showed Ti leaching as well as partial collapse of the mesoporous structure.[36,37] The fresh Nb-EISA and C−Nb-EISA catalysts along with the corresponding spent catalysts after the fourth recycle run and after a 10 h extended run were analyzed by the N_2 physisorption method. As inferred from Table 1 (entries 9−12), no significant changes between the fresh and spent catalysts were observed in the nitrogen physisorption isotherms and pore size distribution, confirming that the catalysts are structurally stable under reaction conditions. Further, no evidence of Si leaching was observed in the spent reaction mixtures providing complementary evidence that the Nb leaching is not due to a loss of the structural integrity of the siliceous support during the reaction. These observations thus clearly demonstrate that inducing hydrophobicity in the pores not only enhances epoxidation rates but also inhibits leaching. This provides guidance for future work in developing new catalyst synthesis methods to achieve optimum hydrophobicity that minimizes catalyst leaching to practically viable levels.

3.4. Proposed Mechanism for Propylene Epoxidation.
Recently, our group[21] and collaborators[38] conducted mechanistic investigations of liquid phase ethylene epoxidation by aqueous hydrogen peroxide catalyzed by niobium silicate. Density functional theory calculations were used to investigate catalytic pathways[38] and probable reasons[21] for hydrogen peroxide decomposition and potential metal leaching. In the present work, the propylene epoxidation was performed under reaction conditions similar to ethylene epoxidation[21,38] using a similar type of Nb incorporated mesoporous silicate as catalyst. We therefore hypothesize that the ethylene epoxidation mechanism can be extended to propylene epoxidation as well. Scheme 1 shows plausible mechanistic pathways for propylene epoxidation based on previous studies.[21,38]

A five-step cycle is proposed. The initial steps consist of adsorption of hydrogen peroxide to the Nb center followed by coordination of propylene to the H_2O_2, resulting in the formation of Nb-hydroperoxide. The H_2O_2 coordinated propylene then undergoes epoxidation via an oxygen atom transfer from the hydroperoxide moiety to the C=C bond of propylene via a transition state.[39] The epoxidation proceeds preferentially as a direct attack of the nucleophilic olefin on an

Table 6. Recycle Study of Nb-EISA (1.9 wt % Nb) and C−Nb-EISA (1.6 wt % Nb) for Propylene Epoxidation[b]

no.	cycle[a]	catalyst amt (mg)	Nb wt %	Y_{PO} mmol (±3%)	P_{PO} (±3%)	S_{EO} % (±3%)	$X_{H_2O_2}$ % (±3%)	$U_{H_2O_2}$ % (±3%)	leaching % (±5%)
1	Nb-EISA	300	1.88	0.926	3274	>99	9.3	>99	6.3
2	R1	284	1.66	1.143	4682	>99	11.3	97.7	6.7
3	R2	278	1.55	1.103	4960	>99	10.8	>99	5.7
4	R3	256	1.46	0.873	4525	>99	8.6	>99	5.2
5	R4	245	1.38	0.748	4279	>99	7.5	>99	5.8
6	C−Nb-EISA	300	1.55	0.552	2305	>99	5.3	>99	2.4
7	R1	278	1.51	0.434	2000	>99	4.3	>99	3.8
8	R2	264	1.45	0.390	1864	>99	3.9	>99	3.7
9	R3	253	1.40	0.393	2152	>99	3.8	>99	3.4
10	R4	241	1.35	0.331	1973	>99	3.3	>99	3.6

[a]"R#" stands for recycle run, and the # (1−4) represents the corresponding number of the recycle run. [b]Reaction conditions: MeOH = 624 mmol, AN = 3 mmol, T = 35 °C, propylene P = 9 bar (maintained constant), t = 3 h, 1400 rpm.

Scheme 1. Proposed Mechanism for Propylene Epoxidation Using Aqueous Hydrogen Peroxide as Oxidant[a]
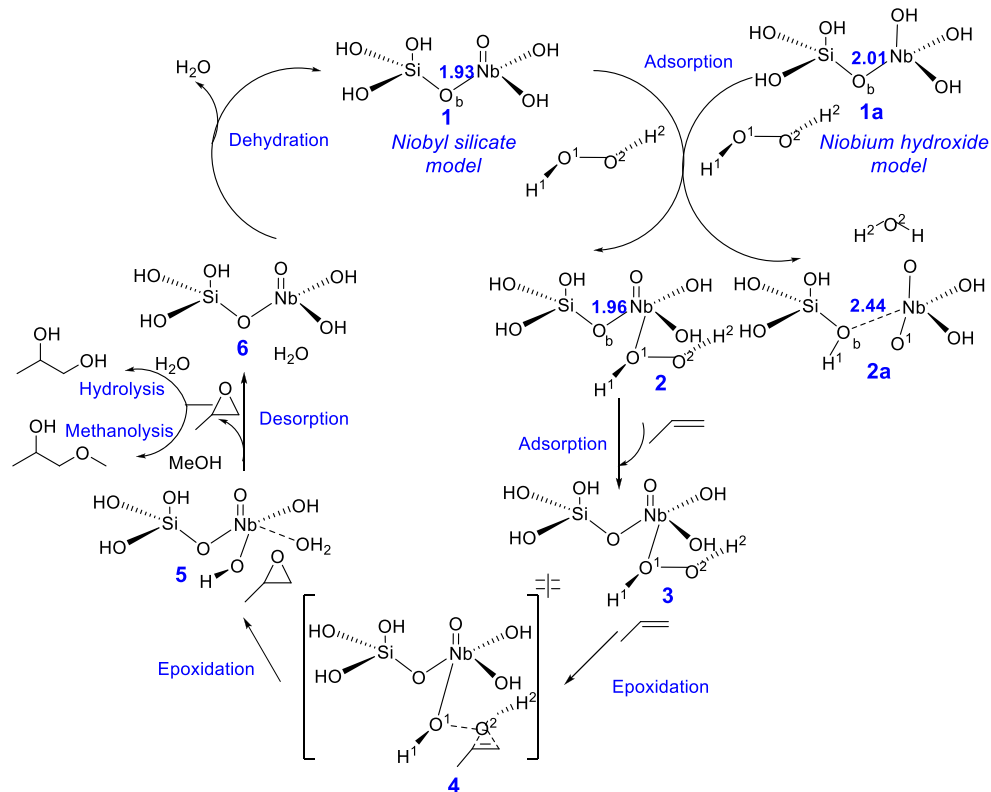
[a]All bond distances are in Å.

electrophilic peroxo oxygen center via a transition state of spiro structure (Sharpless mechanism). Propylene epoxidation follows an electrophilic mechanism in which the $\pi_{C=C}$ bond of the alkene transfers electrons to the σ_{O-O*} peroxo antibond of the Nb-hydroperoxide intermediate and accepts electrons from the $\pi*$ orbital of peroxo oxygen into its (alkene's) $\pi*$ orbital. This electron donation process elongates the O–O bond and eventually leads to its cleavage to form the corresponding epoxide. The epoxidation step to form propylene oxide is the rate-limiting step. The subsequent steps involve desorption of the propylene oxide product followed by dehydration to regenerate the catalyst. If methanol is used as solvent, the propylene oxide can further undergo hydrolysis and solvolysis reactions to form the corresponding byproducts, propylene glycol and isomers of methoxy propanol, respectively. The extent of byproduct formation depends on the Brønsted acidity of the catalyst and the process conditions. In general, higher Brønsted acidity, temperature, and water content enhance byproduct formation.

It is noteworthy that the reaction of the niobium silicate structure with H_2O_2 was modeled in different orientations[21] in order to understand the mechanism of H_2O_2 adsorption (step 1 in Scheme 1), potential H_2O_2 decomposition, and metal leaching. The computational model suggested that Brønsted acidity can induce H_2O_2 decomposition and metal leaching. According to the model, when H_2O_2 is adsorbed on a Lewis acidic site (Nb=O, niobyl silicate model, compound **1** in Scheme 1) in the perpendicular orientation, the process is less exothermic with $\Delta H = -9.1$ kcal/mol (-12.4 kcal/mol for the parallel orientation). However, the model could not predict a pathway for H_2O_2 decomposition when it is bound to niobyl

silicate indicating that Lewis acidic sites show no H_2O_2 decomposition.

In contrast, when H_2O_2 is adsorbed on a Brønsted acidic site (Nb–OH, niobium hydroxide model, compound **1a** in Scheme 1), it readily undergoes decomposition in a highly exothermic process ($\Delta H = -52.0$ kcal/mol), breaking the O^1-O^2 bond and forming water through extraction of the hydroxyl proton to O^2 (compound **2a**, Scheme 1). This process transfers H^1 proton from the O^1 of H_2O_2 to the bridging oxygen (O_b). Dissociation of the O_b–Nb bond (via bond elongation) leads to Nb leaching. Clearly, the ideal catalyst should display predominant Lewis acidity to favor epoxidation and minimal Brønsted acidity to reduce H_2O_2 decomposition and metal leaching. In order to reduce the Brønsted acidity, we hypothesized that catalysts with relatively low Nb content should have more isolated Nb sites (Lewis acid sites) with reduced Brønsted acid sites. A catalyst synthetic technique such as the Evaporation Induced Self-Assembly (EISA) method has been reported to provide improved metal dispersion with relatively low Brønsted acidity.[31] The fact that the Nb-EISA catalysts with enhanced Lewis acidity and reduced Brønsted acidity clearly improves epoxidation yield with reduced leaching lends credence to this proposed mechanism.

4. CONCLUSIONS

Nb-EISA catalysts with low Nb loadings (<2 wt %) exhibit excellent activity for propylene epoxidation displaying virtually total PO selectivity and H_2O_2 utilization toward PO formation with much reduced Nb leaching compared to Nb silicates prepared by impregnation and/or hydrothermal synthesis techniques. This excellent performance is attributed to the

presence of predominantly Lewis acid sites with significantly lower Brønsted acid sites. However, on Nb-EISA catalysts with higher Nb loadings (>3.7 wt %), the PO selectivity and H_2O_2 utilization decrease with increased Nb leaching. This deterioration in performance is attributed to increases, albeit low, in Brønsted acidity at reaction conditions. Carbonized versions of the Nb-EISA improve the performance of such catalysts by increasing pore hydrophobicity that enhances propylene concentration in the pores while inhibiting polar molecules, especially water and the resultant formation of Brønsted acid sites. The Nb-EISA and its carbonized version are both stable and recyclable catalysts. These insights pave the way for rational design of improved propylene epoxidation catalysts.

■ ASSOCIATED CONTENT

ⓢ Supporting Information

The Supporting Information is available free of charge on the ACS Publications website at DOI: 10.1021/acs.iecr.9b03461.

Schematic of experimental unit and figures for characterization of Nb-EISA and C−Nb-EISA (carbonized version) catalyst samples (PDF)

■ AUTHOR INFORMATION

Corresponding Author
*Phone: +1-785-864-2903. Fax: +1-785-864-6051. E-mail: bsubramaniam@ku.edu.

ORCID ⓞ
Bala Subramaniam: 0000-0001-5361-1954

Notes
The authors declare no competing financial interest.

■ ACKNOWLEDGMENTS

■ REFERENCES

(1) Nijhuis, T. A.; Makkee, M.; Moulijn, J. A.; Weckhuysen, B. M. The Production of Propylene Oxide: Catalytic Processes and Recent Developments. *Ind. Eng. Chem. Res.* **2006**, *45*, 3447−3459.

(2) Climent, M. J.; Corma, A.; Iborra, S. Heterogeneous Catalysts for the One-Pot Synthesis of Chemicals and Fine Chemicals. *Chem. Rev.* **2011**, *111*, 1072−1133.

(3) Hayashi, T.; Tanaka, K.; Haruta, M. Selective Vapor-Phase Epoxidation of Propylene over Au/TiO₂ Catalysts in the Presence of Oxygen and Hydrogen. *J. Catal.* **1998**, *178*, 566−575.

(4) Schmidt, F.; Bernhard, M.; Morell, H.; Pascaly, M. HPPO Process Technology: A novel route to propylene oxide without coproducts. *Chim. Oggi* **2014**, *32*, 31−35.

(5) Liu, M.; Ye, X. X.; Liu, Y. Q.; Wang, X. Y.; Wen, Y. Q.; Sun, H. J.; Li, B. J. Highly Selective Epoxidation of Propylene in a Low-Pressure Continuous Slurry Reactor and the Regeneration of Catalyst. *Ind. Eng. Chem. Res.* **2015**, *54*, 5416.

(6) Taramasso, M.; Perego, G.; Notari, B. *Preparation of Porous Crystalline Synthetic Material comprised of Silicon and Titanium Oxide.* U.S. Patent 1983, 4 410 501.

(7) Chen, L. Y.; Chuah, G. K.; Jaenicke, S. Propylene epoxidation with hydrogen peroxide catalyzed by molecular sieves, containing framework titanium. *J. Mol. Catal. A: Chem.* **1998**, *132*, 281−292.

(8) Liu, X. W.; Wang, X. S.; Guo, X. W.; Li, G. Effect of solvent on the propylene epoxidation over TS-1 catalyst. *Catal. Today* **2004**, *93−95*, 505−509.

(9) Lee, H. J.; Shi, T. P.; Busch, D. H.; Subramaniam, B. A greener, pressure intensified propylene epoxidation process with facile product separation. *Chem. Eng. Sci.* **2007**, *62*, 7282−7289.

(10) Zuwei, X.; Zhou, N.; Sun, Y.; Li, K. Reaction-controlled phase-transfer catalysis for propylene epoxidation to propylene. *Science* **2001**, *292*, 1139−1141.

(11) Kamata, K.; Yonehara, K.; Sumida, V.; Yamaguchi, K.; Hikichi, S.; Mizuno, N. *Science* **2003**, *300*, 964.

(12) Weiner, H. *Process for epoxidizing olefins with hydrogen peroxide using supported oxo-diperoxo tungstate catalyst complex.* U.S. PTO 60/999913, 2007.

(13) Lu, X.; Wu, H.; Jiang, J.; He, M.; Wu, V. Selective synthesis of propylene oxide through liquid-phase epoxidation of propylene with H_2O_2 over formed Ti-MWW catalyst. *J. Catal.* **2016**, *342*, 173−183.

(14) Chen, L. Y.; Chuah, G. K.; Jaenicke, S. Propylene epoxidation with hydrogen peroxide catalyzed by molecular sieves containing framework titanium. *J. Mol. Catal. A: Chem.* **1998**, *132*, 281−292.

(15) Chen, C.; Zhao, X.; Chen, J.; Hua, L.; Zhang, R.; Guo, L.; Song, B.; Gan, H.; Hou, Z. Niobium Peroxide-Catalyzed Selective Epoxidation of Allylic Alcohols. *ChemCatChem* **2014**, *6*, 3231−3238.

(16) Ramanathan, A.; Maheswari, R.; Subramaniam, B. Facile Styrene Epoxidation with H_2O_2 over Novel Niobium Containing Cage Type Mesoporous Silicate, Nb-KIT-5. *Top. Catal.* **2015**, *58*, 314−324.

(17) Ahn, S.; Thornburg, N. E.; Li, Z.; Wang, T. C.; Gallington, L. C.; Chapman, K. W.; Notestein, J. M.; Hupp, J. T.; Farha, O. K. Stable metal-organic framework-supported niobium catalysts. *Inorg. Chem.* **2016**, *55*, 11954−11961.

(18) Thornburg, N. E.; Nauert, S. L.; Thompson, A. B.; Notestein, J. M. Synthesis-Structure Function Relationships of Silica-Supported Niobium(V) Catalysts for Alkene Epoxidation with H_2O_2. *ACS Catal.* **2016**, *6*, 6124−6134.

(19) Thornburg, N. E.; Thompson, A. B.; Notestein, J. M. Periodic Trends in Highly Dispersed Groups IV and V Supported Metal Oxide Catalysts for Alkene Epoxidation with H_2O_2. *ACS Catal.* **2015**, *5*, 5077−5088.

(20) Ivanchikova, I. D.; Maksimchuk, N. V.; Skobelev, I. Y.; Kaichev, V. V.; Kholdeeva, O. A. Mesoporous niobium-silicates prepared by evaporation-induced self-assembly as catalysts for selective oxidations with aqueous H_2O_2. *J. Catal.* **2015**, *332*, 138−148.

(21) Yan, W.; Ramanathan, A.; Patel, P. D.; Maiti, S. K.; Laird, B. B.; Thompson, W. H.; Subramaniam, B. Mechanistic Insights for Enhancing Activity and Stability of Nb-incorporated Silicates for Selective Ethylene Epoxidation. *J. Catal.* **2016**, *336*, 75−84.

(22) Turco, R.; Aronne, A.; Carniti, P.; Gervasini, A.; Minieri, L.; Pernice, P.; Tesser, R.; Vitiello, R.; Di Serio, M. Influence of preparation methods and structure of niobium oxide-based catalysts in the epoxidation reaction. *Catal. Today* **2015**, *254*, 99−103.

(23) Tiozzo, C.; Palumbo, C.; Psaro, R.; Bisio, C.; Carniato, F.; Gervasini, A.; Carniti, P.; Guidotti, M. The stability of niobium-silica catalysts in repeated liquid-phase epoxidation tests: A comparative evaluation of in-framework and grafted oxides. *Inorg. Chim. Acta* **2015**, *431*, 190−196.

(24) Ramanathan, A.; Zhu, H.; Maheswari, R.; Thapa, P. S.; Subramaniam, B. Comparative Study of Nb-Incorporated Cubic Mesoporous Silicates as Epoxidation Catalysts. *Ind. Eng. Chem. Res.* **2015**, *54*, 4236−4242.

(25) Nakajima, K.; Baba, Y.; Noma, R.; Kitano, M.; Kondo, J. N.; Hayashi, S.; Hara, M. $Nb_2O_5 \cdot nH_2O$ as a heterogeneous catalyst with water-tolerant Lewis acid sites. *J. Am. Chem. Soc.* **2011**, *133*, 4224−4227.

(26) Jehng, J. M.; Wachs, I. E. Structural chemistry and Raman spectra of niobium oxides. *Chem. Mater.* **1991**, *3*, 100−107.

(27) Jehng, J. M.; Wachs, I. E. Molecular design of supported niobium oxide catalysts. *Catal. Today* **1993**, *16*, 417−426.

(28) Di Serio, M.; Turco, R.; Pernice, P.; Aronne, A.; Sannino, F.; Santacesaria, E. Valuation of $Nb_2O_5 - SiO_2$ catalysts in soybean oil epoxidation. *Catal. Today* **2012**, *192*, 112−116.

(29) Yan, W.; Ramanathan, A.; Ghanta, M.; Subramaniam, B. Towards highly selective ethylene epoxidation catalysts using hydrogen peroxide and tungsten- or niobium-incorporated mesoporous silicate (KIT-6). *Catal. Sci. Technol.* **2014**, *4*, 4433−4439.

(30) Maiti, S. K.; Ramanathan, A.; Thompson, W. H.; Subramaniam, B. Strategies to Passivate Brønsted Acidity in Nb-TUD-1 Enhance Hydrogen Peroxide Utilization and Reduce Metal Leaching during Ethylene Epoxidation. *Ind. Eng. Chem. Res.* **2017**, *56*, 1999−2007.

(31) Ramanathan, A.; Zhu, H.; Maheswari, R.; Subramaniam, B. Remarkable epoxidation activity of neat and carbonized niobium silicates prepared by evaporation-induced self-assembly. *Microporous Mesoporous Mater.* **2018**, *261*, 158−163.

(32) Liu, Y.; Murata, K.; Inaba, M. Synthesis and Catalytic Activity of Niobium-Containing Hexagonal Mesoporous Silica. *Chem. Lett.* **2003**, *32*, 992−993.

(33) Jin, H.; Subramaniam, B. Homogeneous catalytic hydroformylation of 1-octene in CO_2-expanded solvent media. *Chem. Eng. Sci.* **2004**, *59*, 4887−4893.

(34) Pham, H. N.; Anderson, A. E.; Johnson, R. L.; Schwartz, T. J.; O'Neill, B. J.; Duan, P.; Schmidt-Rohr, K.; Dumesic, J. A.; Datye, A. K. Carbon Overcoating of Supported Metal Catalysts for Improved Hydrothermal Stability. *ACS Catal.* **2015**, *5*, 4546−4555.

(35) Steenbergen, K. G.; Kern, J. L.; Wang, Z.; Thompson, W. H.; Laird, B. B. Tunability of Gas-Expanded Liquids under Confinement: Phase Equilibrium and Transport Properties of Ethylene-Expanded Methanol in Mesoporous Silica. *J. Phys. Chem. C* **2016**, *120*, 5010−5019.

(36) Wróblewska, A.; Makuch, E. Studies on the deactivation of Ti-MCM-41 catalyst in the process of allyl alcohol epoxidation. *Pol. J. Chem. Technol.* **2013**, *15*, 111.

(37) Wróblewska, A.; Makuch, E. Regeneration of the Ti-SBA-15 catalyst used in the process of allyl alcohol epoxidation with hydrogen peroxide. *J. Adv. Oxid. Technol.* **2014**, *17*, 44.

(38) Patel, P. D.; Laird, B. B.; Thompson, W. H. A Density Functional Theory Study of Ethylene Epoxidation Catalyzed by Niobium-doped Silica. *J. Mol. Catal. A: Chem.* **2016**, *424*, 1−7.

(39) Di Valentin, C.; Gisdakis, P.; Yudanov, I. V.; Rösch, N. Olefin Epoxidation by Peroxo Complexes of Cr, Mo, and W. A Comparative Density Functional Study. *J. Org. Chem.* **2000**, *65*, 2996−3004.